Measurement of Nucleotide Exchange Rate Constants in Single Rabbit Soleus Myofibrils during Shortening and Lengthening Using a Fluorescent ATP Analog

Ibuki Shirakawa,* Shigeru Chaen,* Clive R. Bagshaw,[†] and Haruo Sugi*
*Department of Physiology, School of Medicine, Teikyo University, Tokyo 173, Japan, and [†]Department of Biochemistry, University of Leicester, Leicester LE1 7RH, England

ABSTRACT   The kinetics of displacement of a fluorescent nucleotide, 2′(3′)-O-[N[2-[[Cy3]amido]ethyl]carbamoyl]-adenosine 5′-triphosphate (Cy3-EDA-ATP), bound to rabbit soleus muscle myofibrils were studied using flash photolysis of caged ATP. Use of myofibrils from this slow twitch muscle allowed better resolution of the kinetics of nucleotide exchange than previous studies with psoas muscle myofibrils (Chaen et al., 1997, *Biophys. J.* 73:2033–2042). Soleus myofibrils in the presence of Cy3-EDA-nucleotides (Cy3-EDA-ATP or Cy3-EDA-ADP) showed selective fluorescence staining of the A-band. The K_m for Cy3-EDA-ATP and the K_d for Cy3-EDA-ADP binding to the myofibril A-band were 1.9 μM and 3.8 μM, respectively, indicating stronger binding of nucleotide to soleus cross-bridges compared to psoas cross-bridges (2.6 μM and 50 μM, respectively). After flash photolysis of caged ATP, the A-band fluorescence of the myofibril in the Cy3-EDA-ATP solution under isometric conditions decayed exponentially with a rate constant of 0.045 $\pm$ 0.007 s^{-1} (n = 32) at 10°C, which was about seven times slower than that for psoas myofibrils. When a myofibril was allowed to shorten with a constant velocity, the nucleotide displacement rate constant increased from 0.066 s^{-1} (isometric) to 0.14 s^{-1} at 20°C with increasing shortening velocity up to 0.1 myofibril length/s (V_{max}, the shortening velocity under no load was ~0.2 myofibril lengths/s). The rate constant was not significantly affected by an isovelocity stretch of up to 0.1 myofibril lengths/s. These results suggest that the cross-bridge kinetics are not significantly affected at higher strain during lengthening but depend on the lower strain during shortening. These data also indicate that the interaction distance between a cross-bridge and the actin filament is at least 16 nm for a single cycle of the ATPase.

INTRODUCTION

When muscle is allowed to shorten and produce external work, the total energy liberated (heat + work) is increased (the Fenn effect; Fenn, 1923, 1924), and the rate of ATP hydrolysis has also been shown to increase with shortening velocity (Kushmerick and Davies, 1969). The mechanism by which muscle modulates the energy output depending on the external work holds some clues to the molecular mechanism of mechanochemical energy transduction. A. F. Huxley (1957) interpreted the Fenn effect by proposing that cross-bridge detachment is relatively slow under isometric conditions, but during contraction, the resulting low or negative mechanical strain of the cross-bridge markedly accelerates the detachment rate. Previously, to study the energy-modulating mechanism at the cross-bridge level, we have devised a method for measuring the nucleotide exchange kinetics of single contracting muscle myofibrils. The displacement rate constant of the prebound fluorescent nucleotide, formed in the presence of Cy3-EDA-ATP, was determined by flash photolysis of excess caged ATP and shown to be strain-dependent (Chaen et al., 1997).

In the present experiments, the rate constants for Cy3-EDA-nucleotide exchange in contracting rabbit soleus muscle myofibrils were measured. Intact slow-twitch muscles have a slower velocity of unloaded shortening and force development than fast-twitch muscles (Close, 1972; Moss, 1982). Three- to 30-fold slower kinetic constants of slow-twitch skinned muscles compared with the fast-twitch skinned muscles have also been reported (Kawai and Schachat, 1984; Poole et al., 1988; Millar and Homsher, 1992; Wang and Kawai, 1996, 1997). Rabbit soleus muscle myofibrils should therefore provide a better preparation to test the utility of the fluorescent nucleotide exchange method, because in our set-up the acquisition is limited by video rate capture (30 Hz). We show that the nucleotide displacement rate constant of soleus muscle myofibrils increased with increasing shortening velocity up to ~50% of the observed V_{max}, indicating a strain-dependent rate constant that limits ATP turnover. However, an imposed lengthening of the myofibril produced no detectable effect on the kinetics of displacement. A preliminary report of related work has been presented (Shirakawa et al., 1998).

MATERIALS AND METHODS

Experimental solutions

The experimental solutions were prepared as described previously (Chaen et al., 1997) and are summarized here. The Ca^{2+}-free rigor solution contained 60 mM *N,N*-bis(2-hydroxyethyl)-2-aminoethanesulfonic acid (BES) (pH 7.1), 53 mM EGTA, 3.2 mM MgCl$_2$, 30 mM dithiothreitol, and

1% β-mercaptoethanol. The Ca^{2+} rigor solution contained 60 mM BES (pH 7.1), 33 mM 1,6-diaminohexane-N,N,N',N'-tetraacetic acid (HDTA), 20 mM EGTA, 20 mM $CaCl_2$, 1.3 mM $MgCl_2$, 30 mM dithiothreitol, and 1% β-mercaptoethanol. Unless otherwise stated, the activating solution contained Ca^{2+} rigor solution plus 5 μM Cy3-EDA-ATP, 5.2 mM caged ATP (Calbiochem, San Diego, CA), and the ATP regenerating reagents (20 mM phosphocreatine (Sigma, St. Louis, MO), 150 units/ml creatine phosphokinase (Sigma)). The free Ca^{2+} concentration in the activating solution was calculated to be ~30 μM. Details of the synthesis of Cy3-EDA-ATP or Cy3-EDA-ADP were described previously and were used as mixed 2', 3' isomers (Chaen et al., 1997). The concentration of Cy3-EDA-ATP or Cy3-EDA-ADP was determined, assuming an absorbance coefficient A_{550} of 150,000 M^{-1} cm^{-1}. Cy3.29-OSu succinimidyl ester was purchased from Amersham Life Science (Pittsburgh, PA). BES, EGTA, and HDTA were from Dojindo Laboratories (Kumamoto, Japan). Other chemicals were of analytical grade.

Preparations of myofibrils

Bundles of muscle fibers (~3 mm in diameter) were dissected from rabbit soleus (slow-twitch) muscles and tied to glass rods, kept in a 50% glycerol solution containing 5 mM potassium phosphate (pH 6.8) and 2 mM EGTA at 4°C overnight, then stored at -20°C after the solution was changed. Myofibrils were prepared by a procedure similar to that of Anazawa et al. (1992). Small strips of muscle fibers (~0.5 mm in diameter and ~5 mm in length) were dissected from the glycerol-extracted soleus muscle fibers, put into the 5 ml of Ca^{2+}-free rigor solution in a test tube, and homogenized (Polytron homogenizer, type PT10/35; Kinematica, Littau/Lucerne, Switzerland) for 20 s at a moderate rotation speed. Myofibrils were then kept in the Ca^{2+}-free rigor solution at 0°C and used on the same day. Myofibrils prepared in this manner had a sarcomere length of ~2.5 μm.

Experimental procedure

The experimental apparatus, procedure, and data analysis used were described in detail previously (Chaen et al., 1997) and are summarized here. A single myofibril was mounted by wrapping its ends around a pair of glass microneedles (elasticity over 200 pN/nm) and held horizontally in an experimental trough (Anazawa et al., 1992). For experiments involving myofibril lengthening or shortening, one glass microneedle was used as a fixed end, and the other end was attached to a piezoelectric actuator (PSt150/7/90, Dr. Lutz Pickelmann, Piezomechanik Optik, Munich, Germany; piezo drive amplifier, M-2617, MES-TEK, Wako, Japan; and function generator/arbitrary wave form generator, HP33120A, Hewlett-Packard, Loveland, CO) to impose a constant-velocity stretch or release of the myofibril preparation. The myofibril fluorescence was observed with the inverted fluorescent microscope (IMT2, SPlan Apo 100× oil immersion objective lens (N.A. 1.4); Olympus, Tokyo, Japan) equipped with a laser scanning unit for confocal microscopy (Insight Plus, scanning rate 120 frames/s, Meridian, Okemos, MI; fluorescence excitation source, argon ion laser, 514.5 nm, Innova 307, Coherent, Santa Clara, CA). Images were recorded with a silicon intensified target camera (C2400–08; Hamamatsu Photonics, Hamamatsu, Japan) and an image processor (Argus 10; Hamamatsu Photonics), and the successive video frames were stored on a personal computer (Power Macintosh 7600/120; Apple Computer Japan, Tokyo) through a frame grabber board (LG3 PCI; Scion, Frederick, MD). Cy3-EDA-nucleotides bound to actomyosin in the myofibril were displaced with ATP generated from caged ATP with a xenon flash lamp apparatus (SA-200E; Eagle Shouji, Tokyo, Japan). Electronic stimulators (SEN-7013 and SEN-3301; Nihon Kohden, Tokyo, Japan) were used to trigger the frame grabber board in the computer, the protective electronic shutter, the flash lamp, and the function generator in the required sequence. The trough temperature was regulated by water circulation through a brass block attached to the trough and another block jacketing the objective. Rate

constants for fluorescent nucleotide displacement from the myofibril on flash photolysis of caged ATP were calculated by the method of Conibear and Bagshaw (1996). A video image sequence of the region around the fluorescent myofibril was captured using National Institutes of Health Image (public domain application written by Wayne Rasband, National Institutes of Health) using a dual time scale controlled by a customized macro program. In experiments involving lengthening or shortening of a myofibril, a constant area was analyzed to include the whole myofibril. In these cases, the bright fluorescence from the section of myofibril wrapped around the needle was blanked off in each frame before analysis so that it did not contribute to the observed fluorescence signal when within the region of interest (e.g., see Fig. 5 B). Previous control experiments in which a myofibril was allowed to contract in the presence of 10 μM Cy3-EDA-ATP, but without flash photolysis, demonstrated that there was no artefact in the intensity profile due to myofibril shortening (Chaen et al., 1997). From the series of video images, the mean fluorescence intensity of the myofibril was computed as a function of time. The data were then analyzed to determine the displacement rate constant by nonlinear least-squares fitting to an exponential function using Kaleidagraph (Synergy Software, Reading, PA).

In experiments involving myofibril shortening or lengthening, immediately after the flash photolysis, ramp signals were generated from the function generator to allow the myofibril to shorten or lengthen at a defined constant velocity. The amount of ramp shortening or lengthening was set at ~10–20% of the initial myofibril length; thereafter the myofibril length was held constant until the myofibril fluorescence diminished to zero. Typically myofibrils as prepared had a sarcomere length of ~2.5 μm. In the case of lengthening experiments, the myofibril was initially allowed to shorten to ~2.1 μm before flash photolysis of caged ATP, so that the final sarcomere length after 10–20% stretch remained below 2.5 μm. Displacement rate constants of Cy3-EDA-nucleotides in the shortening or lengthening phase were estimated from the initial part of the fluorescence decay, which corresponded to the ramp shortening or stretch, together with the final end-point signal. Only one measurement was made from each myofibril. In all cases, the rate of photobleaching was negligible compared with the displacement rate. Likewise, there was no evidence of photobleaching caused by the xenon flash.

RESULTS

We have shown previously that displacement of fluorescent nucleotides by flash photolysis of caged ATP is useful for measuring the ATP turnover rate constants of single contracting myofibrils (Chaen et al., 1997). However, in the previous experiments using psoas muscle myofibrils, the temperature was lowered to 8°C to slow down events of interest so that they could be resolved at standard video rate capture. With soleus muscle myofibrils data could be obtained at higher temperatures (20°C).

Cy3-EDA-nucleotide as a substrate for the cross-bridge cycle in soleus myofibrils

Fig. 1, A and C, shows video images of isolated soleus muscle myofibrils in a solution containing 5 μM Cy3-EDA-ATP and 5 μM Cy3-EDA-ADP, respectively. Both nucleotides showed selective fluorescence staining of the A-band with a reduced fluorescence at the M-line. Fluorescence intensities of the myofibrils as a function of Cy3-EDA-ATP and Cy3-EDA-ADP concentration are shown in Fig. 1, B and D, respectively. The K_m and K_d for the nucleotide
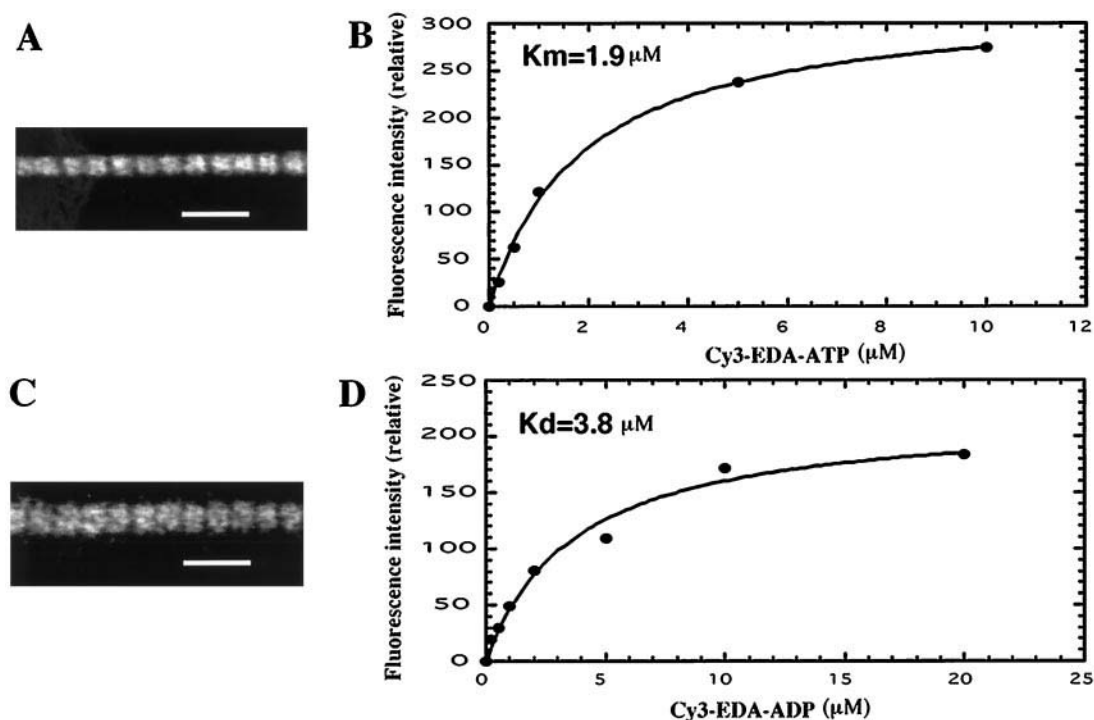
FIGURE 1   Fluorescence from a soleus myofibril in the Ca^{2+}-free rigor solution containing Cy3-EDA-ATP or Cy3-EDA-ADP. (*A*) A video image of a myofibril in the solution containing 5 μM Cy3-EDA-ATP. Scale bar, 10 μm. (*B*) Dependence of fluorescence intensity of a myofibril on the concentration of Cy3-EDA-ATP. The K_m corresponding to the fitted hyperbola is 1.9 μM. (*C*) A video image of a myofibril in the solution containing 5 μM Cy3-EDA-ADP. Scale bar, 10 μm. (*D*) Dependence of fluorescence intensity of a myofibril on the concentration of Cy3-EDA-ADP. The K_d corresponding to the fitted hyperbola is 3.8 μM.

binding were 1.9 μM and 3.8 μM, respectively. These data indicate tighter binding of nucleotide to soleus muscle cross-bridges compared with the psoas muscle cross-bridges, especially for Cy3-EDA-ADP (K_m for Cy3-EDA-ATP, 2.6 μM; K_d for Cy3-EDA-ADP, ~50 μM; Chaen et al., 1997). At the 5 μM Cy3-EDA-ATP used in subsequent experiments, ~72% of the cross-bridges are initially occupied by Cy3-EDA-nucleotide. However, competition from caged ATP (K_i = 1.6 mM; Sleep et al., 1994) would reduce this percentage to ~50%.

Fig. 2 *A* shows selected video images of the displacement of Cy3-EDA-nucleotide bound to cross-bridges in the myofibril by flash photolysis of caged ATP during isometric contraction at 10°C. Fig. 2 *B* shows the exponential decay of the mean Cy3 fluorescence intensity with time. To detect possible deviations from a single exponential at early time points, the data are also presented on a logarithmic time scale (Fig. 2 *C*). Quantitative analysis of the fluorescence decay curve of Fig. 2, *B* and *C*, yielded a rate constant of 0.043 s^{-1}, which is about seven times slower than that of psoas myofibrils (0.3 s^{-1}) at 8°C (Chaen et al., 1997).

An attempt was made to follow directly the displacement of Cy3-EDA-ADP from soleus cross-bridges by the flash photolysis of caged ATP. The displacement rate constant was ~3.2 ± 2.3 s^{-1} (n = 5) at 10°C. In the case of rabbit

psoas myofibrils, the displacement of Cy3-EDA-ADP was too fast to be determined by this method (Chaen et al., 1997). These data suggest that, in the presence of Cy3-EDA-ATP, the predominant nucleotide complex is not an A.M.Cy3-EDA-ADP complex and that Cy3-EDA-ADP release is not rate limiting.

The Cy3-EDA-nucleotide displacement rate constant from soleus myofibrils under isometric conditions was also measured at 20°C; histograms for the rate constants at 20°C and 10°C for individual myofibrils are shown in Fig. 3. The rate constants for a few myofibrils appeared to fall outside the main distribution in having values of ~0.12 s^{-1} (n = 3) at 20°C and 0.07 s^{-1} (n = 3) at 10°C. These groups may relate to the fast-twitch type isoform in the soleus myofibrils, as has been shown by Wang and Kawai (1996b). They have reported that 11% of rabbit soleus fibers are of the fast-twitch type, as judged by their higher characteristics frequencies in sinusoidal length-tension analysis. In Fig. 3, the rate constants of slow-type muscle myofibrils at 20°C and 10°C were 0.066 ± 0.010 s^{-1} (n = 34) and 0.045 ± 0.007 s^{-1} (n = 32), respectively. In the experiment described below during lengthening and shortening contractions at 20°C, we excluded the data in which the isometric phase had a rate constant higher than 0.1 s^{-1} so as to avoid inclusion of fast-type myofibril isoforms.
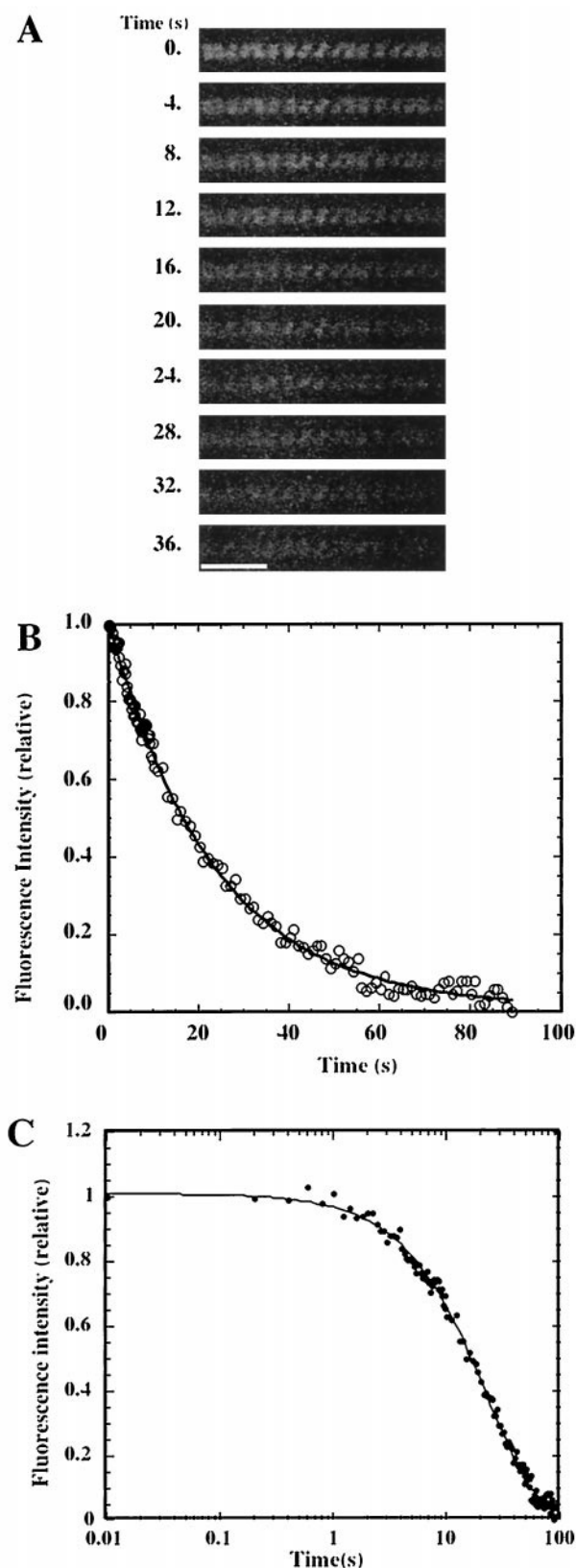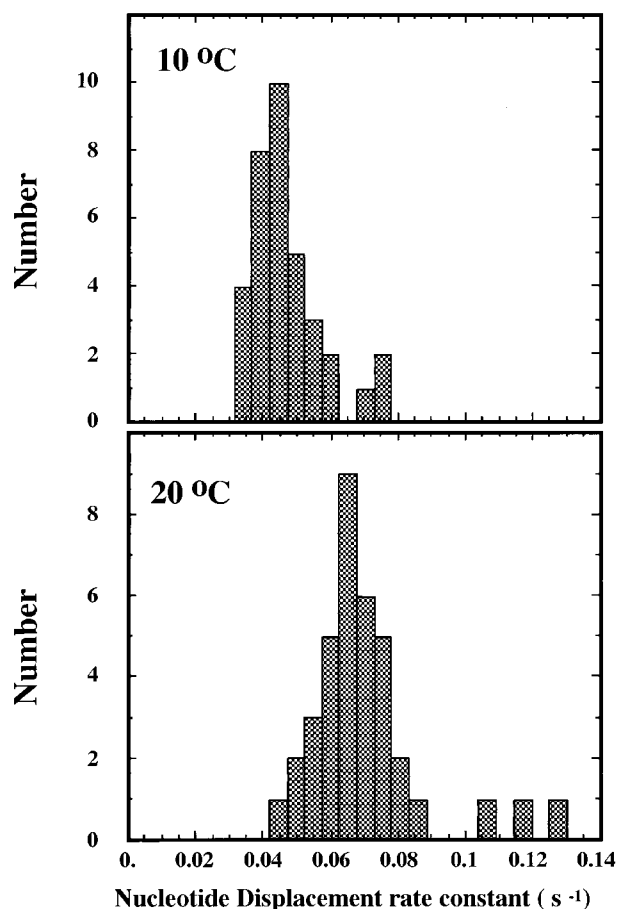
FIGURE 3 The temperature dependence of the rate constant for nucleotide displacement from soleus myosfibrils under isometric conditions. The top and bottom panels show the histogram of the rate constants at 10°C and 20°C, respectively.

Effect of mechanical constraints on the nucleotide displacement rate constant

The fluorescence decay from prebound Cy3-EDA-nucleotide was measured when the myofibril was allowed to shorten or forced to stretch after the flash photolysis of caged ATP. Experiments were performed at 20°C. Fig. 4 *A* shows representative video images of a fluorescent myofibril that was allowed to shorten for 20% of its myofibril length (Fig. 5 *A*) at 0.1 myofibril length/s and then kept isometric. In these experiments triggering of the frame grabber coincided with the initiation of the shortening phase. When the fluorescence intensity profile corresponding to the shortening phase was fitted to a single exponential

FIGURE 2 A typical experiment showing the displacement of Cy3-EDA nucleotide (formed in the presence of 5 μM Cy3-EDA-ATP) from a soleus myofibril by flash photolysis of 5.2 mM caged ATP under isometric

conditions at 10°C. (*A*) Selected video images of a myofibril, showing the displacement of fluorescent nucleotide from the A-band. Scale bar, 10 μm. (*B*) Quantitative analysis of the displacement of Cy3-EDA nucleotide. The data points were fitted to a single exponential, which gave a rate constant of 0.043 s^{-1}. (*C*) The same data presented on a logarithmic time scale.
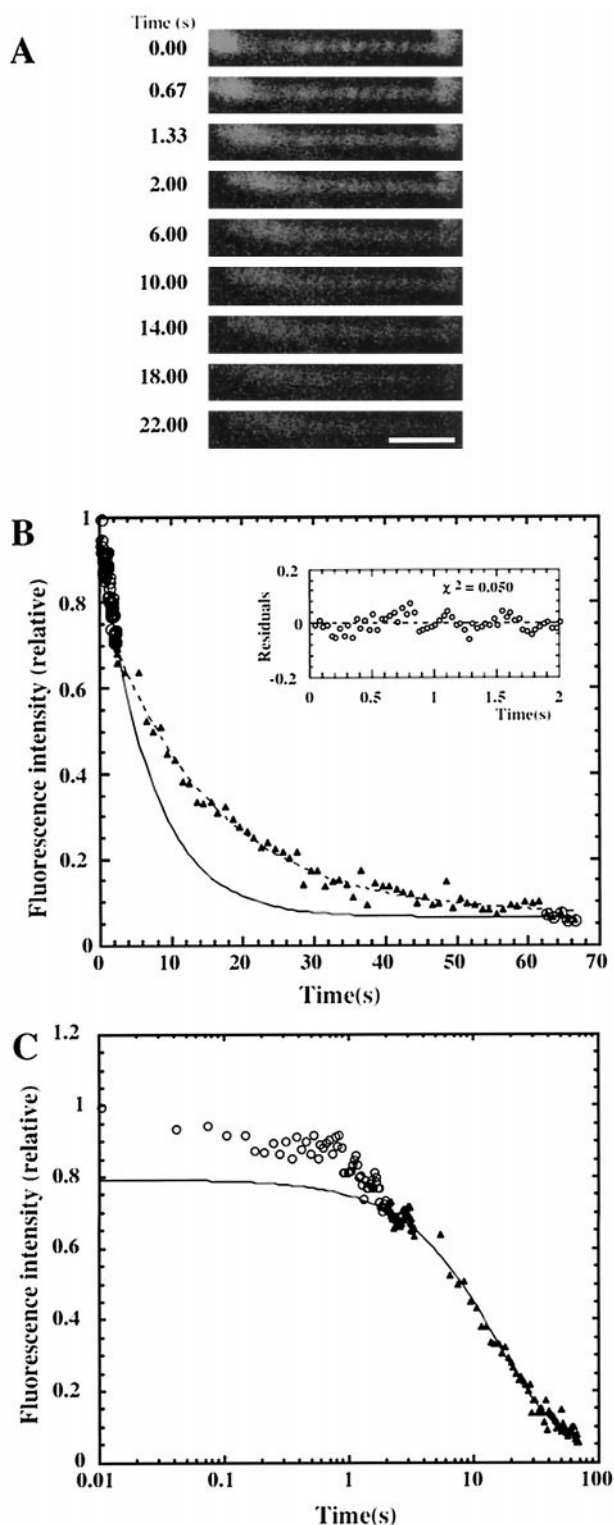
FIGURE 4 A typical experiment showing the displacement of Cy3-EDA nucleotide (formed in the presence of 5 μM Cy3-EDA-ATP) from a soleous myofibril by flash photolysis of caged ATP during shortening. The myofibril preparation was initially bathed in activating solution. (*A*) Selected video images of the myofibril after flash photolysis of caged ATP, during shortening at 0.10 myofibril lengths/s (time 0 to 2 s), and then subsequently while it was held isometrically. Scale bar, 10 μm. (*B*)

(Fig. 4 *B*), the rate constant (0.14 s^{-1}) deviated from that of the isometric part of the profile (0.067 s^{-1}). This deviation is more clearly observed on a logarithmic time scale (Fig. 4 *C*). To check that the change in rate constant corresponds to the shortening process and is not an artefact of the flash, a delayed shortening experiment was devised. In this experiment (Fig. 5), a myofibril was held isometrically for 2 s after the flash, then allowed to shorten for 2 s, before returning to the isometric condition. Fig. 5 *A* shows representative video frames from the experiment, and Fig. 5 *B* indicates the masking procedure used to remove the contribution of the fluorescence from the needles (as employed in all shortening/lengthening experiments). Also in this experiment, video frames were collected just before the flash and during shutter closure, to check for any instantaneous drop in fluorescence. Data from the different phases were fitted to single exponential functions using a common end point corresponding to the frames recorded after 60 s, when the fluorescent image had practically disappeared. Fig. 5 *C* shows the complete intensity profile, and Fig. 5 *D* shows an enlargement of the early phases. After recovery of the SIT camera from shutter closure, the initial isometric phase fit to a rate constant of 0.52 s^{-1}. On shortening the displacement markedly accelerated to 0.14 s^{-1}, then slowed to 0.52 s^{-1} when the myofibril was held isometric again. Extrapolation of the first isometric phase back to the time of the flash indicates that an intensity change of less than a 5% occurred because of photobleaching or an unresolved rapid displacement phase.

Experiments were also carried out in which the myofibril was forced to lengthen after flash photolysis of caged ATP. The lengthening velocity that could be applied was limited by the tendency for the myofibril to break at values more negative than −0.1 myofibril length/s. Fig. 6 shows a typical experiment conducted in a manner analogous to that of the experiment depicted in Fig. 4, but with an imposed lengthening rather than shortening. While there was some deviation of the early data points from the single-exponential fit to the isometric phase, there was no clear effect on lengthening. Certainly there is no indication of a slowing of the rate constant by a factor of 2, which would be the expected result if the strain dependence were linear over the velocity range of ±0.1 myofibril length/s.

Quantitative analysis of the displacement of Cy3-EDA-nucleotide during shortening. The solid and broken curves represent fitting of the data (*open circles* and *closed triangles*) to a single exponential curve, which gave rate constants of 0.14 s^{-1} and 0.067 s^{-1} for the shortening and isometric phases, respectively. The final points of isometric contraction were used as an end point for the decay of the shortening phase. The inset shows residuals between the experimental values and the fitted curve during the shortening phase. (*C*) Same data plotted on a logarithmic time scale to show deviation of the data points recorded during shortening from the isometric fit.
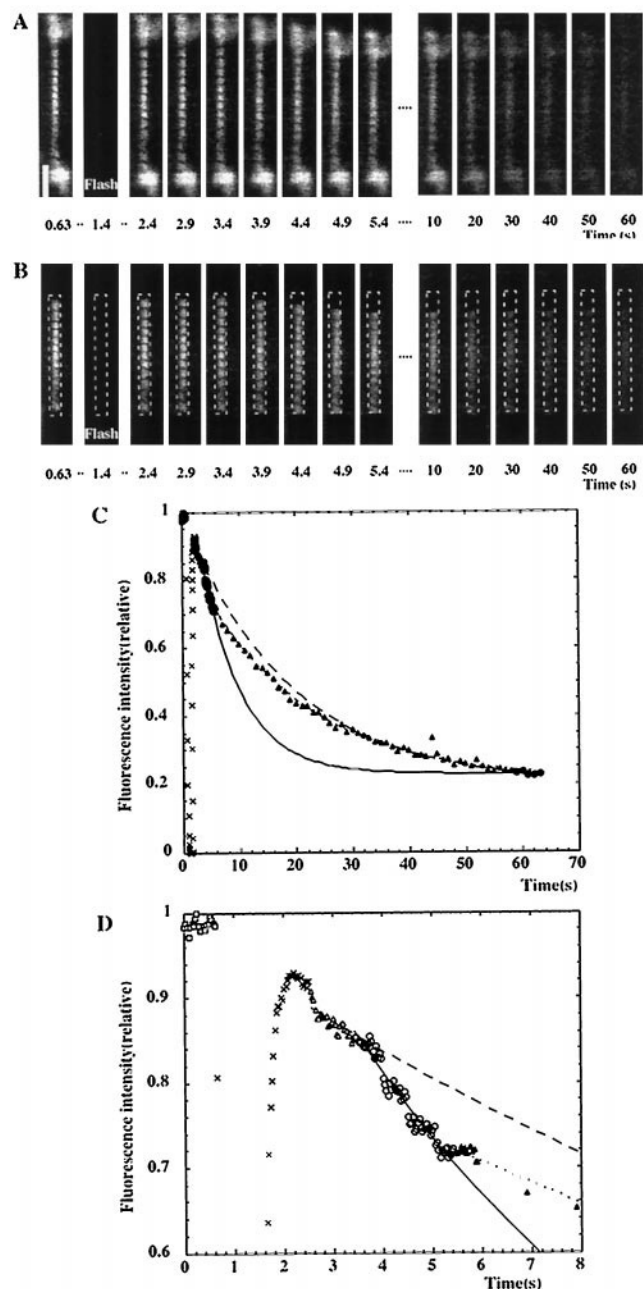
FIGURE 5   A delayed shortening experiment showing that the displacement of Cy3-EDA nucleotide is accelerated during the shortening phase. (*A*) Selected video images of the myofibrils in the presence of 5 μM Cy3-EDA-ATP. The xenon lamp flash occurred at 1.4 s. The myofibril was held isometric until 3.4 s, then it was allowed to shorten at 0.056 Lo/sec until 5.4 s, before being held isometric again. Scale bar, 10 μm. (*B*) The same video images as in *A*, after erasure of the needle fluorescence and selection of a rectangular region of interest for analysis. (*C* and *D*) Quantitative analysis of the displacement of Cy3-EDA-nucleotide. The broken (0.052 s^{-1}), solid (0.14 s^{-1}), and dotted (0.052 s^{-1}) curves represent single exponential fits to the data for the first isometric (*open triangles*), shortening (*open circles*), and second isometric phases (*closed triangles*), respectively. The first isometric data points were fitted from 2.54 s because of the lag after the shutter opened and the unstable data points around 2.5 s. The same end-point intensity (final five points) was used for all three curves. Square and crossed symbols show the intensity before

In Fig. 7 the observed nucleotide displacement rate constants for the soleus myofibrils are plotted against the velocity of myofibril shortening or lengthening. The rate constant increased from 0.066 s^{-1} to 0.14 s^{-1} as the shortening velocity was increased from zero to 0.1 myofibril length/s. The maximum shortening velocity of the myofibril under the solution conditions used was estimated to be ~0.2 myofibril length/s by the observation that myofibrils became slack when the imposed shortening velocity exceeded 0.2 myofibril length/s. On the other hand, lengthening by up to 0.1 myofibril length/s had no detectable effect.

DISCUSSION

When a soleus myofibril is incubated with Cy3-EDA-ATP, the fluorescent nucleotide binds selectively to myosin cross-bridges. Under the conditions of the experiment (5 μM Cy3-EDA-ATP), the predominant cross-bridge states are likely to be A.M., A.M.Cy3-EDA-ADP.P$_i$ and M.Cy3-EDA-ADP.P$_i$ together with some A.M.caged ATP (see below for arguments). On flash photolysis, the excess ATP released will bind to vacant myosin sites, effectively displacing the fluorescent nucleotide at a rate that reflects the Cy3-EDA nucleotide product release steps plus a possible contribution from back-dissociation to release Cy3-EDA-ATP. Whereas the latter process is negligible in the case of myosin alone, the extent of back-dissociation in the presence of actin is less clear. Sleep (1981) found up to ~25% of the bound nucleotide could be released as ATP in myofibrils, while Houadjeto et al. (1992) interpreted this as release from noncompetent sites and concluded that >98% of the active-site-bound nucleotide proceeded via the hydrolysis and turnover route. Either interpretation indicates that the displacement rate is dominated by turnover events. Note that the observed rate constant for displacement reflects a weighted sum for the actin-activated and nonactivated myosin pathways. During shortening, the release of cross-bridge strain is likely to accelerate the actin-activated ATPase of attached cross-bridges. The experiments described in this paper offer some quantitative conclusions.

In general the kinetics of displacing Cy3-EDA-nucleotides from soleus muscle myofibrils compared with that of psoas muscle myofibrils (Chaen et al., 1997) yielded rate constants that were smaller by around sevenfold under comparable conditions. This ratio is consistent with that for psoas and soleus fiber steady-state ATPase rates reported by Potma et al. (1994). They found that the ATP turnover rate constant, measured by NADH breakdown through a coupled enzyme assay, was 2.1 s^{-1} for psoas fibers and 0.28 s^{-1} for soleus fibers at 15°C. The absolute values of the rate

flash photolysis and during shutter closure, respectively. In *D* the time scale is expanded to emphasize the acceleration in rate during shortening.
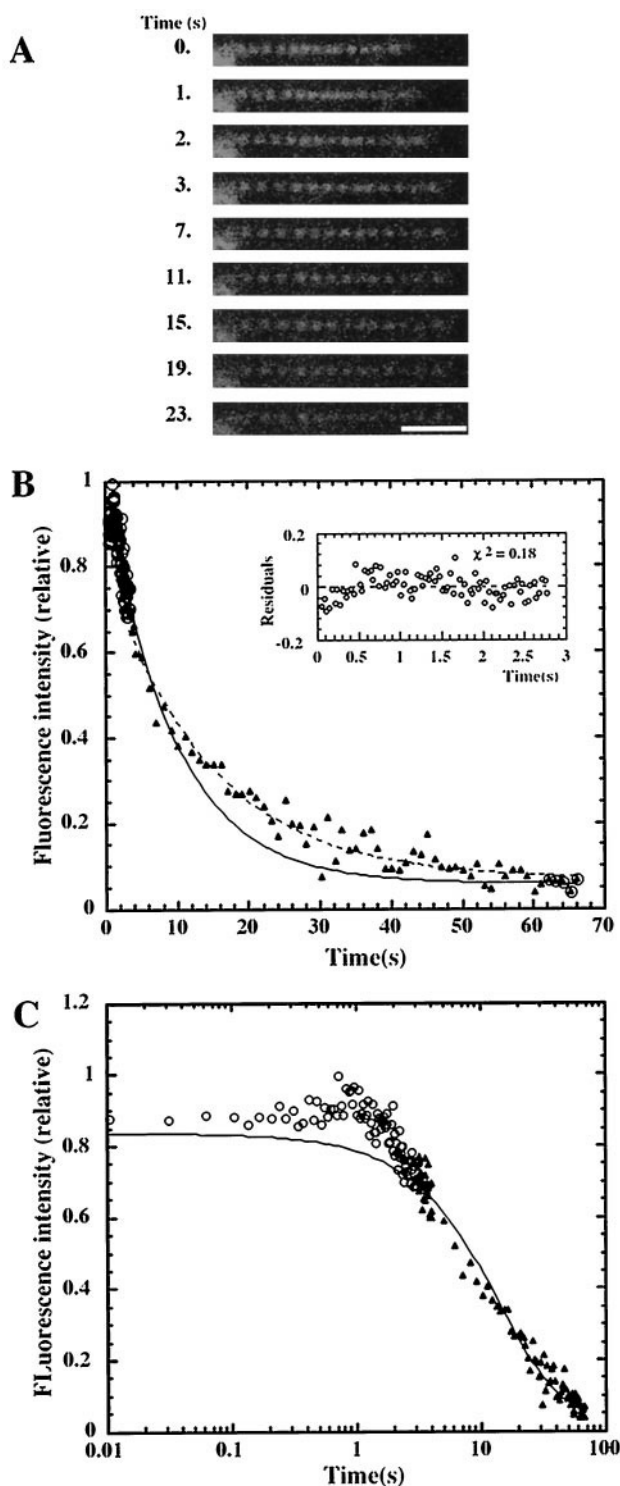
FIGURE 7 Relation between the observed Cy3-EDA-nucleotide (formed in the presence of 5 μM Cy3-EDA-ATP) displacement rate constants and the velocity of shortening and lengthening. The myofibril preparations were bathed in activating solution and induced to shorten or lengthen as described in Figs. 4 and 6. Negative values of the velocity represent the lengthening. The error bar at zero velocity represents the standard deviation of the rate constant during isometric contraction (Fig. 3). The data were from different myofibril preparations.

constants found using Cy3-EDA-ATP as a substrate in our study with either muscle type are, however, about five to seven times lower than those of Potma et al. (1994), who used ATP. This difference is probably due to the properties of Cy3-EDA-ATP, which has been reported to slow down the cross-bridge cycling rate (Chaen et al., 1997). The kinetic parameters of myosin and actomyosin with Cy3-EDA-ATP in solution are within a factor of 2–4 of those of ATP (Eccleston et al., 1996; Conibear et al., 1996). Ishijima et al. (1998) reported that the unitary cross-bridge displacements induced by Cy3-EDA-ATP were 12 nm, under conditions in which ATP gave a value of 15 nm, while the second-order rate constant for Cy3-EDA-ATP binding was about half that of ATP.

The competition from caged ATP reduces the amplitude of the initial fluorescence signal by reducing the initial occupancy of the Cy3-EDA-nucleotides, but it should have little effect on their displacement kinetics by ATP once photolysis occurs. The residual nonphotolyzd caged ATP, however, may reduce the sliding velocity of the unloaded shortening velocity (cf. Thirlwell et al., 1995). The combined effect of Cy3-EDA-nucleotides and caged ATP inhibition probably accounts for the fourfold slower maximum sliding velocity we observed compared with literature data (Moss, 1982). A similar factor was noted previously for

FIGURE 6 A typical experiment showing the displacement of Cy3-EDA-nucleotide (formed in the presence of 5 μM Cy3-EDA-ATP) from a soleous myofibril by flash photolysis of caged ATP during lengthening. (*A*) Selected video images of the myofibril after flash photolysis of caged ATP, during lengthening at 0.067 myofibril lengths/s (time 0 to 3 s), and then subsequently while being held isometrically. Scale bar, 10 μm. (*B*) Quantitative analysis of the displacement of Cy3-EDA-nucleotide during lengthening. The solid and broken curves represent single exponential fits to give rate constants of 0.09 s^{-1} and 0.07 s^{-1} for the lengthening (*open circles*) and isometric (*closed triangles*) phases, respectively. The final points of isometric contraction were used as an end point of the decay for the lengthening phase. The inset shows residuals between the experimental values and the fitted curve during the lengthening phase. (*C*) Same data plotted on a logarithmic time scale to show deviation of the data points recorded during lengthening from the isometric fit.
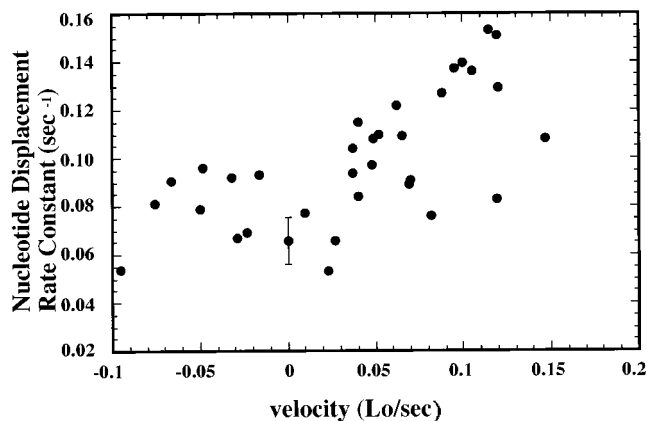
psoas muscle myofibrils (Chaen et al., 1997). The observation that the ATPase and shortening velocity were reduced in unison suggests that mechanochemical coupling is maintained during the turnover of Cy3-EDA-ATP by myofibrils.

The rate constants for Cy3-EDA-nucleotide displacement for slow-type muscle myofibrils, under isometric conditions at 20°C and 10°C, were 0.066 ± 0.010 s^{-1} ($n = 34$) and 0.045 ± 0.007 s^{-1} ($n = 32$), respectively, giving a ratio of ~1.5, which is somewhat smaller than the Q_{10} of the ATP hydrolysis rate (1.8) in rabbit psoas fast-twitch fibers (Zao and Kawai, 1994). According to Wang and Kawai (1996a), the temperature sensitivity of the kinetic constants of soleus slow twitch fibers is similar to those of psoas fast twitch fibers, apart from the smaller absolute values in the slow-twitch fibers.

The binding of Cy3-EDA-ADP is markedly tighter in the case of soleus myofibrils compared with psoas ($K_d = 3.8$ μM compared to 50 μM, respectively). Similar observations for soleus muscle fibers have been made by Wang and Kawai (1996b) and Horiuti et al. (1997). Wang and Kawai (1996b) showed that the MgADP association equilibrium constant for rabbit soleus muscle fibers derived from their sinusoidal analysis was eight times that for rabbit psoas fibers, while Horiuti et al. (1997) reported that the decrease in rigor tension by the addition of ADP was more marked in soleus than psoas muscle fibers. Our data suggest that Cy3-EDA-nucleotide retains the fundamental properties of the natural substrate in showing tighter binding to soleus compared with psoas muscle cross-bridges. Nevertheless, the observed displacement rate of Cy3-EDA-ADP cross-bridges in myofibrils (3.5 s^{-1} at 10°C) is more than an order of magnitude faster than that for the predominant nucleotide state(s) induced by Cy3-EDA-ATP. This is in accord with the findings of Lionne et al. (1995) and Barman et al. (1998), who conclude that P$_i$ release is rate limiting in myofibrils. On the other hand, Wang and Kawai (1997) conclude that an isomerization step involving an A.M.*ADP to A.M.ADP transition is rate limiting. However, our result is not necessarily in conflict with the latter, because the A.M.*ADP state is not significantly populated when ADP is added back to the rigor A.M state. Solution studies, at least, suggest that Cy3-EDA-ATP is rapidly hydrolyzed by myosin alone to give a products burst comparable to the phosphate burst with ATP (Shimada et al., 1997), i.e., the predominant nucleotide state in the myofibril is likely to be M.ADP.P$_i$ in equilibrium with its actin-bound state.

The combined measurement of Cy3-EDA-ATP turnover and shortening allows a limit to be placed on the unitary displacement of a cross-bridge per ATP hydrolysis cycle. During shortening at a V_{max} of 0.2 length/s, a myosin filament translates past an actin filament at 250 nm/s in a half-sarcomere. In 1 s only $(1 - \exp(-0.1)) = 0.1$ (i.e., 10%) of the cross-bridges have completed a turnover cycle, based on the Cy3-nucleotide displacement rate constant

(Fig. 7). In a single myosin half-filament this fraction corresponds to ~30 myosin heads (out of 300). Given a 2:1 ratio of actin:myosin filaments in cross section, on average each actin filament is driven by a total of 15 cross-bridges during 1 s of shortening, and thus on average each myosin cross-bridge translates the actin filament by at least $250/15 = 16$ nm per cycle. It follows that the time a cross-bridge remains attached during filament translation is $\leq 16/250 = 0.064$ s, and therefore attached rate constants must exceed 15 s^{-1}. This yields a very low duty ratio such that during shortening at V_{max} less that $0.1/15$ ($= 0.66\%$) of the cross-bridges are attached at any point in time. This calculation supports a previous conclusion based on more disparate literature data (Bagshaw, 1993). The calculated interaction distance of 16 nm would be increased by the coincidental simultaneous operation of two or more cross-bridges on one actin from one myosin half-filament, which would increase nucleotide turnover without affecting the sliding velocity. Loss of bound Cy3-EDA-nucleotide through basal myosin turnover and back-dissociation to free Cy3-EDA-ATP would also increase the calculated interaction distance by the active heads. On the other hand, the distance would be overestimated if sliding were preferentially driven by the released ATP and Cy3-EDA-nucleotide did not faithfully report on the behavior of the average myosin head.

The increase in displacement rate constant during shortening velocities up to 0.1 myofibril length/s fits with the concept of the Huxley (1957) model in which low or negative strain favors detachment and thus speeds up the overall cycling time. Another observation supporting this conclusion is that MgADP dissociates more rapidly from negatively strained cross-bridges than from positively strained ones (Dantzig et al., 1991). On the other hand, an imposed lengthening did not appear to affect the displacement kinetics. However, the range of the imposed lengthening was limited in our experiments by breakage of the myofibril. A very low rate of ATP splitting with high tension on lengthening of a muscle has been observed by Curtin and Davies (1975). They showed that the rate of ATP turnover measured by the amount of inorganic phosphate (P$_i$) release of dinitrofluorobenzene (DNTB)-treated muscle was lower during lengthening than during shortening. Similarly, Homsher et al. (1997) have found that the rate of force decline after P$_i$ release from caged P$_i$ in fibers was little affected at higher strain during lengthening compared with those during shortening.

In summary, the experiments using soleus myofibrils confirmed the usefulness of the nucleotide exchange method in revealing that the energy-modulating mechanism depends on the strain in the cross-bridges. Although the absolute rate constants appear to be reduced by up to fourfold with Cy3-EDA-ATP as an analog, key features of mechanochemical coupling appear to be retained.

REFERENCES

Anazawa, T., K. Yasuda, and S. Ishiwata. 1992. Spontaneous oscillation of tension and sarcomere length in skeletal myofibrils. Microscopic measurement and analysis. *Biophys. J.* 61:1099–1108.

Bagshaw, C. R. 1993. Muscle Contraction, 2nd Ed. Chapman and Hall, London.

Barman, T., M. Brune, C. Lionne, N. Piroddi, C. Poggesi, R. Stehle, C. Tesi., F. Travers, and M. R. Webb. 1998. ATPase and shortening rates in frog fast skeletal myofibrils by time-resolved measurements of protein-bound and free P_i. *Biophys. J.* 74:3120–3130.

Chaen, S., I. Shirakawa, C. R. Bagshaw, and H. Sugi. 1997. Measurement of nucleotide release kinetics in single skeletal muscle myofibrils during isometric and isovelocity contractions using fluorescence microscopy. *Biophys. J.* 73:2033–2042.

Close, R. 1972. Dynamic properties of mammalian skeletal muscle. *Physiol. Rev.* 52:129–197.

Conibear, P. B., and C. R. Bagshaw. 1996. Measurement of nucleotide exchange kinetics with isolated synthetic myosin filaments using flash photolysis. *FEBS Lett.* 380:13–16.

Conibear, P. B., D. S. Jeffreys, C. K. Seehra, R. J. Eaton, and C. R. Bagshaw. 1996. Kinetic and spectroscopic characterization of fluorescent ribose-modified ATP analogs upon interaction with skeletal muscle myosin subfragment 1. *Biochemistry.* 35:2299–2308.

Curtin, N. A., and R. E. Davies. 1975. Very high tension with very little ATP breakdown by active skeletal muscle. *J. Mechanochem. Cell Motil.* 3:147–154.

Dantzig, J. A., M. G. Hibberd, D. R. Trentham, and Y. E. Goldman. 1991. Cross-bridge kinetics in the presence of MgADP investigated by photolysis of caged ATP in rabbit psoas muscle fibers. *J. Physiol. (Lond.)*. 432:639–680.

Eccleston, J. F., K. Oiwa, M. A. Ferenczi, M. Anson, J. E. T. Corrie, A. Yamada, H. Nakayama, and D. R. Trentham. 1996. Ribose-linked sulfoindocyanine conjugates of ATP: Cy3-EDA-ATP and Cy5-EDA-ATP. *Biophys. J.* 70:A159.

Fenn, W. O. 1923. A quantitative comparison between the energy liberated and the work performed by the isolated sartorius muscle of the frog. *J. Physiol. (Lond.).* 58:175–203.

Fenn, W. O. 1924. The relation between the work performed and the energy liberated in muscular contraction. *J. Physiol. (Lond.).* 58: 373–395.

Homsher, E., J. Lacktis, and M. Regnier. 1997. Strain-dependent modulation of phosphate transients in rabbit skeletal muscle fibers. *Biophys. J.* 72:1780–1791.

Horiuti, K., N. Yagi, and S. Takemori. 1997. Mechanical study of rat soleus muscle using caged ATP and x-ray diffraction: high ADP affinity of slow cross-bridges. *J. Physiol. (Lond.).* 502.2:433–447.

Houadjeto, M., F. Travers, and T. Barman. 1992. Ca^{2+}-activated myofibrillar ATPase: transient kinetics and the titration of its active sites. *Biochemistry.* 31:1564–1569.

Huxley, A. F. 1957. Muscle structure and theories of contraction. *Prog. Biophys. Biophys. Chem.* 7:255–318.

Ishijima, A., H. Kojima, T. Funatsu, M. Tokunaga, H. Higuchi, H. Tanaka, and T. Yanagida. 1998. Simultaneous observation of individual ATPase and mechanical events by a single myosin molecule during interaction with actin. *Cell.* 92:161–171.

Kawai, M., and F. H. Schachat. 1984. Differences in the transient response of fast and slow skeletal muscle fibers: correlation between complex modulus and myosin light chain. *Biophys. J.* 45:1145–1151.

Kushmerick, M. J., and R. E. Davies. 1969. The chemical energetics of muscle contraction. II. The chemistry, efficiency and power of maximally working sartorius muscles. *Proc. R. Soc. Lond. Biol.* 174:315–353.

Lionne, C., M. Brune, M. R. Webb, F. Travers, and T. Barman. 1995. Time resolved measurements show that phosphate release is the rate limiting step on myofibrillar ATPases. *FEBS Lett.* 364:59–62.

Millar, N. C., and E. Homsher. 1992. Kinetics of force generation and phosphate release in skinned rabbit soleus muscle fibers. *Am. J. Physiol.* 262:C1239–C1245.

Moss, R. L. 1982. The effect of calcium and magnesium on the maximum velocity of shortening in skinned skeletal muscle fibres of the rabbit. *J. Muscle Res. Cell Motil.* 3:295–311.

Poole, K. J. V., G. Rapp, Y. Maeda, and R. S. Goody. 1988. The time course of changes in the equatorial diffraction pattern from different muscle types on photolysis of caged ATP. *Adv. Exp. Med. Biol.* 226: 391–404.

Potma, E. J., I. A. van Graas, and G. J. M. Stienen. 1994. Effects of pH on myofibrillar ATPase activity in fast and slow skeletal muscle fibers of the rabbit. *Biophys. J.* 67:2404–2410.

Shimada, T., N. Sasaki, R. Ohkura, and K. Sutoh. 1997. Alanine scanning mutagenesis of the switch 1 region in the ATPase site of *Dictyostelium discoideum* myosin II. *Biochemistry.* 36:14037–14043.

Shirakawa, I., S. Chaen, C. R. Bagshaw, and H. Sugi. 1998. Measurement of nucleotide release kinetics in contracting rabbit soleus muscle myofibrils using a fluorescent ATP analogue. *J. Muscle Res. Cell Motil.* 19:444.

Sleep, J. A. 1981. Single turnovers of adenosine 5′-triphosphate by myofibrils and actomyosin subfragment 1. *Biochemistry*, 20:5043–5051.

Sleep, J. A., C. Herrman, T. Barman, and F. Travers. 1994. Inhibition of ATP binding to myofibrils and acto-myosin subfragment 1 by caged ATP. *Biochemistry.* 33:6038–6042.

Thirlwell, H., J. A. Sleep, and M. A. Ferenczi. 1995. Inhibition of unloaded shortening velocity in permeabilized muscle fibres by caged ATP compounds. *J. Muscle Res. Cell Motil.* 16:131–137.

Wang, G., and M. Kawai. 1996a. Temperature and phosphate effects on the elementary steps of the cross-bridge cycle in rabbit soleus slow-twitch muscle fibers. *Biophys. J.* 70:A265.

Wang, G., and M. Kawai. 1996b. Effects of MgATP and MgADP on the cross-bridge kinetics of rabbit soleus slow-twitch muscle fibers. *Biophys. J.* 71:1450–1461.

Wang, G., and M. Kawai. 1997. Force generation and phosphate release steps in skinned rabbit soleus slow-twitch muscle fibers. *Biophys. J.* 73:878–894.

Zao, Y., and M. Kawai. 1994. Kinetic and thermodynamic studies of the cross-bridge cycle in rabbit psoas muscle fibers. *Biophys. J.* 67: 1655–1668.